Journal of Applied Polymer Science

Electroconductive performance of polypyrrole/graphene nanocomposites synthesized through *in situ* emulsion polymerization

Syed Muhammad Imran, Godlisten N. Shao, M. Salman Haider, Nadir Abbas, Manwar Hussain, Hee Taik Kim

Department of Fusion Chemical Engineering, College of Engineering Sciences, Hanyang University, Ansan Gyeonggi 426-791, Republic of Korea

Correspondence to: M. Hussain (E-mail: manwarh@hanyang.ac.kr) and H. T. Kim (E-mail: khtaik@yahoo.com or khtaik@hanyang.ac.kr)

ABSTRACT: The present study demonstrates a modified *in situ* emulsion polymerization (EP) approach convenient for the formation of polypyrrole/graphene (PPy/GN) nanocomposites with harnessed conductivities. A series of PPy/GN nanocomposites were prepared by loading different weight percent (wt %) of GN during *in situ* EP of pyrrole monomer. The polymerization was carried out in the presence of dodecyl benzene sulfonic acid, which acts as an emulsifier and protonating agent. The microstructures of the nanocomposites were studied by scanning electron microscopy, transmission electron microscopy, X-ray diffraction, Fourier transform infrared, X-ray photoelectron spectroscopy, UV–vis spectroscopy, Raman spectroscopy, photoluminescence spectroscopy and thermogravimetric analyses. The electrical conductivities of the nanocomposite pellets pressed at different applied pressures were determined using four probe analyzer. The electrical conductivities of the nanocomposites were considerably enhanced as compared to those of the individual PPy samples pressed at the same pressures. An enhanced conductivity of 717.06 S m^{-1} was observed in the sample with 5 wt % GN loading and applied pressure of 8 tons. The results of the present study signify that the addition of GN in the PPy polymer harnesses both electrical and thermal properties of the polymer. Thus, PPy/GN nanocomposites with superior properties for various semiconductor applications can be obtained through direct loading of GN during the polymerization process. © 2014 Wiley Periodicals, Inc. J. Appl. Polym. Sci. **2015**, *132*, 41800.

KEYWORDS: applications; composites; conducting polymers; emulsion polymerization; surfactants

Received 12 August 2014; accepted 22 November 2014

DOI: 10.1002/app.41800

INTRODUCTION

Graphene (GN) has received a considerable attention since its discovery in 2004 due to its outstanding electronic, mechanical and thermal properties. It represents a new class of materials that are only one atom thick and with its two dimensional all sp^2-hybridized carbon exhibits high conductivity, high surface area and good mechanical properties, comparable to or even better than that of carbon nanotubes (CNT). In case of GN, the charge carriers can travel thousands of inter atomic distances without scattering. Introducing GN into a polymer matrix could appreciably improve the mechanical, thermal and electrical properties of the polymer.[1–4] The composites of GN with different polymers can be obtained through simple chemical procedures such as *in situ* chemical or electrochemical polymerization and non-covalent functionalization. The exfoliated GN possesses a large surface area and could form stronger interactions with the polymer matrix than that of tubular CNT resulting in the superior thermal and electrical properties.[5]

Meanwhile, conductive polymers have been widely researched due to their unique morphology and structure, which influence their physical and electrochemical properties. They are the class of polymeric materials with conjugated unsaturated bonds at the main chains and the combination of these polymers with various carbon materials facilitates the formation of composites suitable for different electrical and electronic applications. The formed composites are widely applied as solid state electrodes for batteries, electrolyte capacitors, shielding materials, corrosion protection, light emitting diodes, solar cells, and chemical sensors. Among various conductive polymers, polypyrrole (PPy) is the most extensively studied polymer because of its high electrical conductivity, environmental stability, and relative ease of synthesis.[6–9] PPy is a heterocyclic aromatic organic compound composed of five-membered ring (C_4H_4NH) with a wide range of applications in electronic and optical devices, chemical and electrochemical sensors, electrochromic devices, actuators and field emission applications.[2] Predominantly, PPy can be prepared by electrochemical polymerization or chemical oxidative

polymerization of the pyrrole monomer. Nevertheless, the harsh conditions during the polymerization process result in the lowering of the electrical conductivities of the resulting polymer suggesting that a polymer with a high electrical conductivity obtained by polymerization must be synthesized under mild conditions.[10]

Several researchers have reported the synthesis of PPy/GN nanocomposites using different synthesis techniques. Manvel *et al.*[11] synthesized PPy/GN nanocomposites by *in situ* polymerization of pyrrole in the presence of strong acid (1*M*, HCl) resulting in modest values of electrical conductivities. Wang *et al.*[12] reported the synthesis of PPy/sulfonated GN nanocomposites through *in situ* doping polymerization using ammonium peroxodisulfate (APS) which is a very strong oxidizing agent. The maximum reported electrical conductivity of the nanocomposites with 50 wt.% sulfonated GN was 5000 S m^{-1}. Amaike *et al.*[10] synthesized polypyrrole by EP using hydroxypropyl cellulose and reported the electrical conductivity of the synthesized polymer as high as 2000 S m^{-1}. These reports indicate that the electrical conductivity, thermal stability and morphology of PPy is largely influenced by two main factors: (1) polymerization conditions which include selection of solvent, temperature, reaction time and oxidant and (2) the category of dopant used during the polymerization (graphene, APS, graphene oxide etc.). Thus, dopants influence the electrical conductivity and the mechanism of charge transport of the polymer. Indeed, the profound relationship between the conductivity, morphology and the chain structure of the polymer has been confirmed in numerous reports.[5,13–15]

In the present report PPy/GN nanocomposites with different weight percent (wt %) of GN were exquisitely synthesized by adopting a simple and reproducible *in situ* EP route. The polymerization experiment of PPy was carried out in the presence of a functionalized protonic acid, dodecyl benzene sulfonic acid (DBSA); which acts as an emulsifier and protonating agent. A comparative study of the electrical conductivities, pressing pressure and GN content was also carried out through forming pellets of PPy/GN nanocomposites at different pressing pressures. To the best of our knowledge, few studies have reported electrical properties of conductive polymers obtained by EP from their individual monomers. However, a systematic evaluation of the electrical properties of PPy/GN nanocomposites has not previously been reported.

EXPERIMENTAL

Materials

All chemical reagents used in this study were of analytical laboratory grade purchased from different sources and used without further purification. Graphene was procured from MK nano, Canada. Pyrrole (98+ %) was bought from Alfa Aesar, USA while Ferric chloride hexahydrate ($FeCl_3.6H_2O$) was purchased from Junsei Chemical, Japan. Dodecyl benzene sulfonic acid (DBSA) was obtained from Sigma–Aldrich, USA.

Synthesis of PPy/GN Nanocomposites

GN with different wt % ranging from 1 to 5% was dispersed in 50 mL deionized (DI) water and sonicated for 30 min in order to exfoliate the GN layers. After the sonication 1.67 g pyrrole was added to each of the GN suspensions and stirred for 1 h at 300 rpm. In the separate flasks three different solutions were prepared by adding 1.74 g DBSA and 15.5 g $FeCl_3.6H_2O$ in 100 mL DI water each. These solutions were added into the pyrrole/GN solutions (1–5 wt %) and stirred for 4 h in order to allow the polymerization reaction to proceed. Black powder was collected by filtration and washed with DI water several times to remove impurities such as $FeCl_3$, free DBSA and un-reacted pyrrole, once the polymerization reaction was completed. Nanocomposites were then dried at 60°C in a vacuum oven for 24 h.

Characterization

X-ray diffraction (XRD) measurements were performed using a Rigaku rotating anode X-ray Diffractometer (D/MAX-2500/PC, Rigaku, Japan) equipped with a Cu Kα radiation source ($\lambda = 0.15418$ nm) at an accelerating voltage of 50 kV and current of 100 mA. Fourier transform infrared (FTIR) spectroscopic measurements of nanocomposite pellets were performed using a Nicolet 6700 with a diamond probe (Thermo Fisher Scientific, MA) within the range of 4000–500 cm^{-1}. A VG scienta, R-3000 X-ray photoelectron spectroscope (XPS) was used to analyze the chemical nature of the nanocomposites. The UV–visible spectra were recorded using an Optizen 2120 (Perkin Elmer Lambda 35UV, South Korea) spectrophotometer. RENISHAW (RM 1000) Raman microscope was used for recording Raman spectra of the samples. Raman spectra were recorded using He-Ne laser beam with wavelength of 632.8 nm, between 800 and 2000 cm^{-1}. An HORIBA JOBIN YVON, USA (FL-1039/40) with PMT detector was essentially used to measure Photoluminescence (PL) spectra of the samples and the excitation wavelength was 397 nm. Morphologies of the samples were studied by High Resolution transmission electron microscopy (HRTEM, JEM-2100F, JEOL, Japan) and Scanning electron microscopy (SEM, JEOL JSM-6330F, Japan).

Thermogravametric analysis (TGA, TA Instruments, Q500, USA) of the polymer nanocomposites was performed at a heating rate of 20°C min^{-1} under nitrogen environment. Electrical conductivities of the nanocomposite pellets were measured at room temperature using collinear 4 probe apparatus (CMT-SR2000N, Chang Min, South Korea) with typical probe spacing s∼1 mm. In this method, current is supplied via a pair of current leads. The voltage drop across the impedance was measured by a separate pair of leads. Thus, the voltage drop in the current carrying wires was prevented from being added to the actual value. An average value was reported from five measurements. The pellets were prepared by compressing nanocomposites into a press (Auto M-NE, H 3891, CARVER, USA) for 10 min with a diameter of 10 mm and thickness of 3–4 mm under pressure of 2, 4, 6, and 8 tons.

RESULTS AND DISCUSSIONS

Generally, *in situ* EP technique has some advantages over other polymerization techniques. During this process the polymerization is essentially carried out under relatively mild conditions and therefore polymers with high molecular weight can be yielded in a convenient and directly useful form. Also the heat

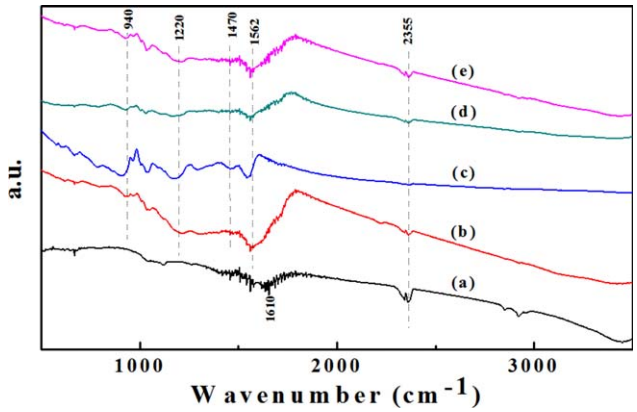

Figure 1. FTIR spectra of GN (a), PPy (b) and PPy/GN composites with GN concentration of 1 wt %, (c) 2 wt %, (d) and 5 wt % (e). [Color figure can be viewed in the online issue, which is available at wileyonlinelibrary.com.]

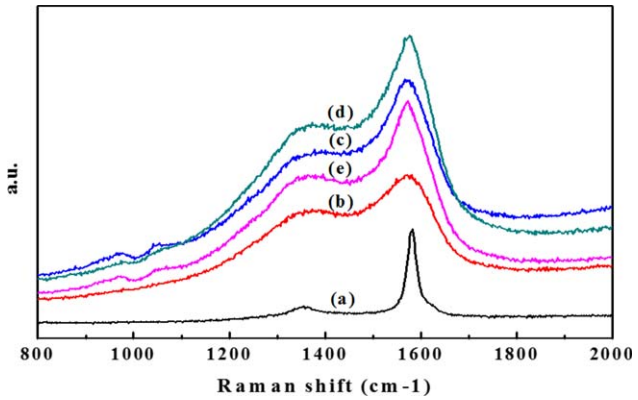

Figure 3. Raman spectroscopy of GN (a), PPy (b), and PPy/GN composites with GN concentration of 1 wt %, (c) 2 wt %, (d) and 5 wt % (e). [Color figure can be viewed in the online issue, which is available at wileyonlinelibrary.com.]

can be controlled due to the presence of water during polymerization process. However, the synthesized polymer needs to be purified vigorously from the surfactant after the polymerization reaction is completed. To date, extensive studies have been attempted to investigate the physicochemical properties of PPy obtained under different polymerization conditions of the pyrrole monomer.[16–20] During synthesis of the composite, surfactants, reducing agents and dopants can largely influence the electrical properties, morphology and thermal properties of the final product. In the present study a modified EP technique was used to obtain PPy/GN nanocomposites with different wt. % of GN using GN and DBSA as doping agents. The electrical conductivities of the resulted nanocomposites were examined at different pressing pressures.

FTIR spectra of GN, PPy, and PPy/GN nanocomposites are displayed in Figure 1. For GN [Figure 1(a)] the band appears at 1590 cm^{-1} which corresponds to C—C skeleton vibration of carbon ring in graphene. The band at 2355 cm^{-1} is related with C═O stretching mode.[21–23] In case of PPy the characteristic peaks at 1562 and 1470 cm^{-1} are attributed to the antisymmetric and symmetric ring stretching vibration. These peaks are also present in case of nanocomposites, indicating the formation of PPy/GN nanocomposites. The absorption peak at 1214 and 940 cm^{-1} represents the bipolaran structure as a result of DBSA doping in PPy.[18,24] Additionally, Figure 2(a–c) shows the wide region XPS spectra of GN, PPy, and PPy/GN (5%) as representative samples. It can be seen that the nitrogen peak is absent in GN but is present in PPy and PPy/GN nanocomposites. The intensity of carbon peak is much higher in case of GN as compared to PPy and PPy/GN nanocomposites.

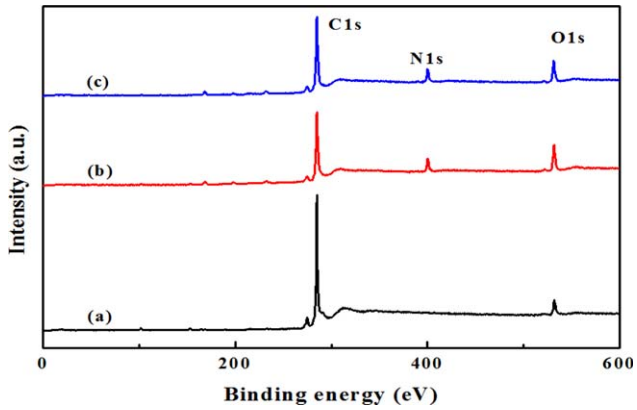

Figure 2. Wide region XPS spectra of GN (a), PPy (b), and PPy/GN composites with GN concentration of 5 wt % (c). [Color figure can be viewed in the online issue, which is available at wileyonlinelibrary.com.]

Raman spectra of GN, PPy, and PPy/GN nanocomposites are depicted in Figure 3. GN [Figure 3(a)] exhibits two peaks, D band at 1356 cm^{-1} which corresponds to the first order Raman scattering of E_2g vibrational mode and G band at 1582 cm^{-1} is related to the vibration of SP^2- hybrided carbon.[17] Typical peaks of PPy are located at 1572 and 1360 cm^{-1} [Figure 3(b)]. In case of PPy/GN nanocomposites two peaks at 972 and 1042 cm^{-1} are attributed to the doped structure of PPy suggesting the interaction of GN in with the PPy matrix.[3,12,20]

The XRD patterns of GN, PPy, and PPy/GN nanocomposites are presented in Figure 4. The GN diffraction peak (002) at $2\theta = 26.5°$ is prominent.[12,23,25] The diffraction pattern of pure PPy displays a broad diffraction peak from $2\theta = 15°$ to 30° depicting the amorphous structure of the polymer. The XRD diffractograms of the PPy/GN nanocomposites are presented in Figure 4(b–d). The shifting of the broad peak of the polymer with increasing wt % of GN can clearly be noticed. This signifies the possible interaction of PPy and GN and perhaps a π–π stacking that occurred between the PPy chains and GN sheets.[12,17,23]

The UV–vis spectra of GN, PPy and PPy/GN nanocomposite (5 wt %) are displayed in Figure 5. Typical GN absorption bands are observed at 235 and 260 nm and are attributed to the electronic configuration in GN.[26] Two absorption bands for PPy at 255 nm and a broad band at 500 nm correspond to the π–π^* transition of the pyrrole ring and the conjugated structure of PPy respectively. In case of the PPy/ GN nanocomposite spectra, a shift of the broad band towards lower wavelength i.e. 465 nm is noticeable. This shift is ascribed to the transition from the

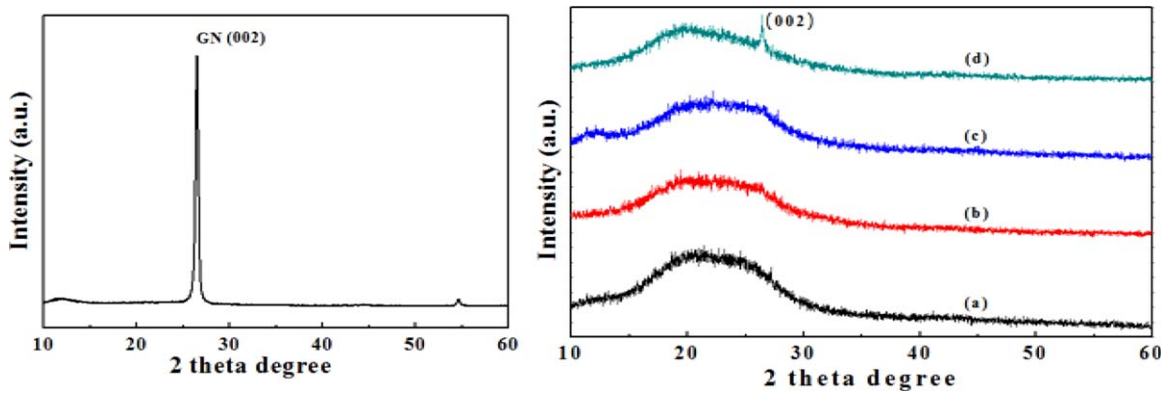

Figure 4. XRD Patterns of GN and PPy (a), PPy/GN composites with GN concentration of 1 wt % (b), 2 wt % (c), and 5 wt % (d). [Color figure can be viewed in the online issue, which is available at wileyonlinelibrary.com.]

valence band to anti-bonding polaron state and it also suggests that the energy gap between the π and π^* is increased due to the strengthening of the conjugated π-bond caused by the interaction between PPy and GN.[3,27]

It was formerly reported that intrachain or interchain carrier pairs are formed during optical excitations. Excitations play a great part in controlling the optical properties of conjugated polymers such as polypyrrole. Therefore, photoluminescence (PL) would be an ideal method to study the carriers and their movements in polymer matrices.[28] Figure 6(A) shows the PL spectra of GN, PPy and PPy/GN nanocomposites with different GN wt %. In each case, broad spectra were registered at 460–450 nm. PL spectra of PPy/GN nanocomposites are very similar to that of PPy sample but their intensities are rather lower than that of PPy. The emission intensities of the nanocomposites were gradually decreased with increasing the GN contents. These PL quenching experiments indicate that the electrons can be conducted between the conducting polymer and GN incorporated in the PPy.[29] This phenomenon is further clarified in Figure 6(B) revealing a subsequent decrease of the emission intensities with increasing the GN content. The efficient quenching of the PL emission allows fast charge separation and slow charge recombination and therefore the nanocomposites might be appropriate for various semiconductor applications.[30,31] Thus, it can be inferred that an efficient charge transfer occurs between the PPy and GN interface.

Figure 7 compiles the TEM images of GN, PPy, and PPy/GN nanocomposites. It can be seen that GN sheets are very thin, transparent, and stalked on each other [Figure 7(a)]. The morphology of PPy is shown in Figure 7(b) and reveals the presence of uniform granular shaped solid nano-spheres. These granular shapes of PPy have also been observed in the samples obtained using naphthalene sulfonic acid and *p*-dodecylbenzene sulfonic acid as surfactants and dopants.[32] PPy/GN nanocomposites [Figure 7(c–e)] show sheet like structures which are completely different from those of pure PPy. This is due to the fact that the polymerization reaction is carried out in the presence of

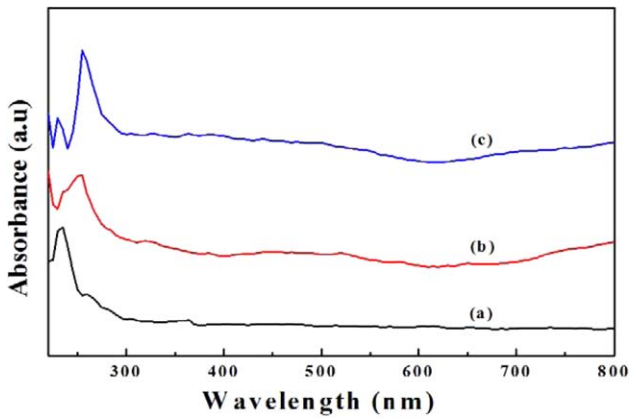

Figure 5. UV–vis absorption spectra of GN (a), PPy (b) and PPy/GN composites with GN concentration of 5 wt % (c). [Color figure can be viewed in the online issue, which is available at wileyonlinelibrary.com.]

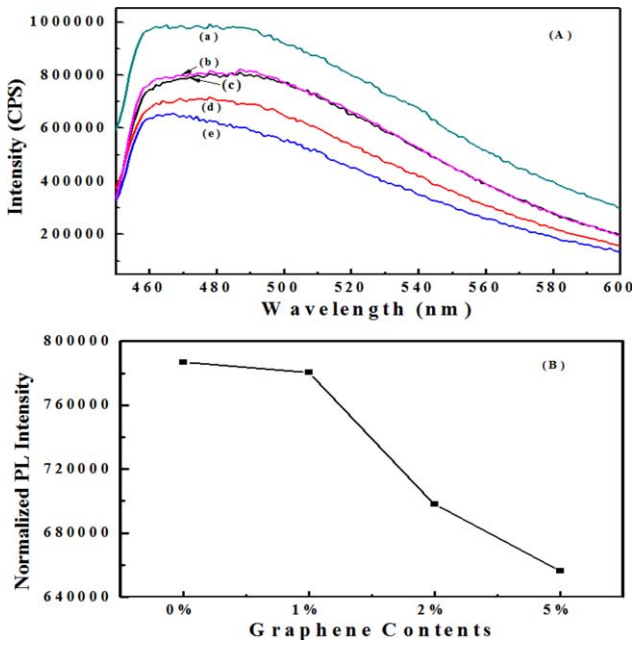

Figure 6. (A) Photoluminescence spectra of GN (a), PPy (b) and PPy/GN composites with GN concentration of 1 wt % (c) 2 wt % (d) and 5 wt % (e); (B) Normalized PL intensity for different GN contents in PPy. [Color figure can be viewed in the online issue, which is available at wileyonlinelibrary.com.]

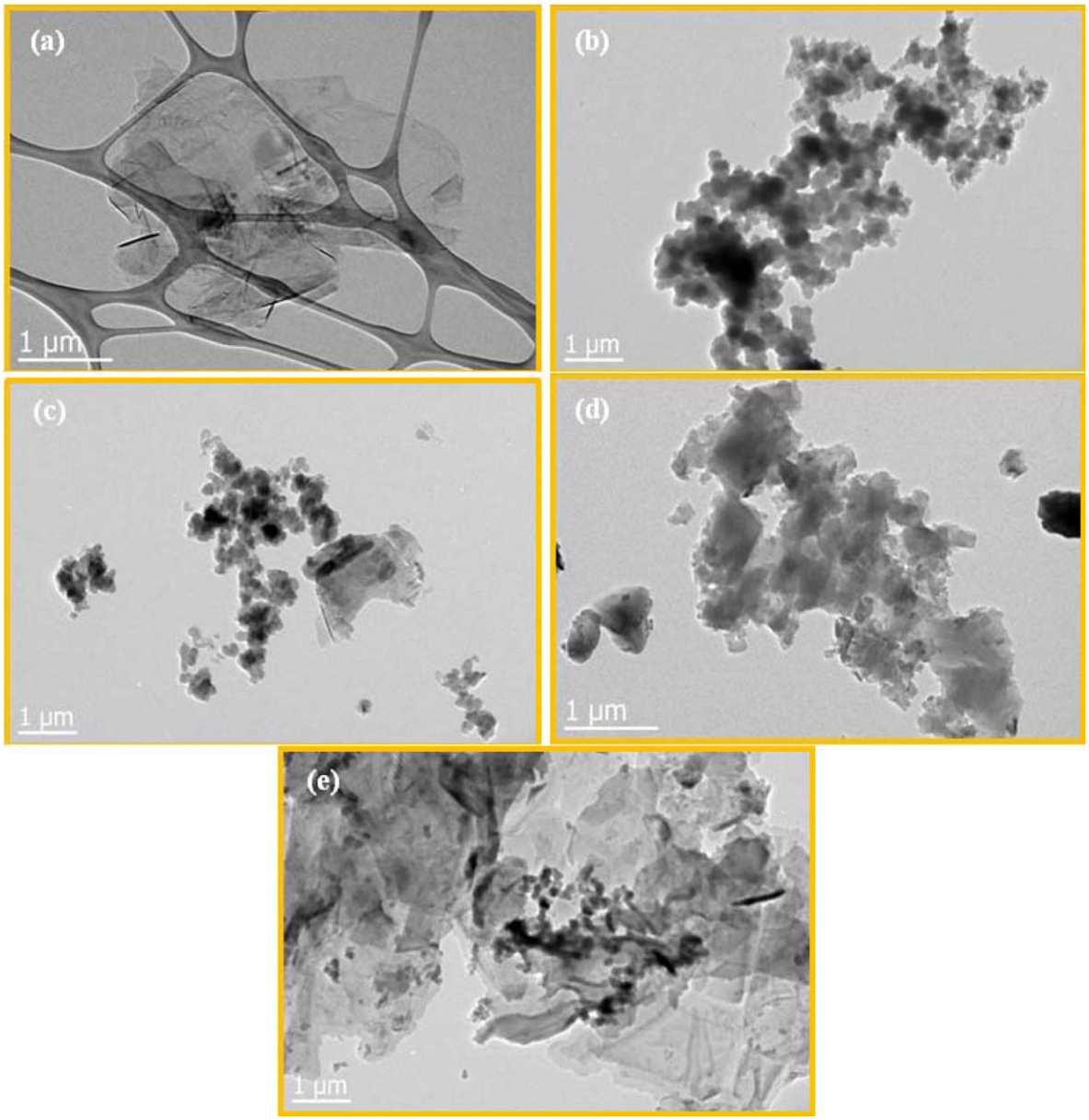

Figure 7. TEM images of GN (a), PPy (b) and PPy/GN composites with GN concentration of 1 wt %, (c) 2 wt %, (d) and 5 wt % (e). [Color figure can be viewed in the online issue, which is available at wileyonlinelibrary.com.]

GN sheets.[33] The mechanism of the polymerization of pyrrole on GN is explained by Xu *et al.*[1] Pyrrole monomers first get absorbed onto the surface of GN sheets through π–π interaction, van der Waal's forces and hydrogen bonding. As the polymerization reaction proceeds, PPy layers form and coat the surface of GN sheets during the *in situ* EP. It is noteworthy that GN sheets are uniformly distributed in PPy and no GN agglomerates can be seen in the TEM images. Uniform distribution of GN in PPy enhances the thermal and electrical properties of the resulting nanocomposites.

Figure 8 presents the SEM images of GN, PPy and PPy/GN nanocomposites. Figure 8(a) shows that the GN nano sheets were well exfoliated and had a clean and uniform surface[1,17] while a continuous chain structure of PPy can be seen in Figure 8(b). Figure 8(c–e) shows the morphology of PPy/GN nanocomposites with 1, 2, and 5 wt % GN respectively. Presence of GN during the polymerization of pyrrole monomer strongly affected the morphology of the resulting PPy and sheet like morphology of the final nanocomposites was obtained. In the case of the nanocomposites; GN serves as a template for the formation of PPy/GN nanostructures.[3,33] This can also be confirmed by the TEM images of the nanocomposites in Figure 7.

TGA curves of GN, PPy, and PPy/GN nanocomposites are shown in Figure 9. GN showed high thermal stability since only 14% of total weight loss was registered at 800°C. PPy showed a total weight loss of ~97% at 800°C signifying that the thermal stability of PPy at elevated temperatures is undoubtedly low. However, there is a huge thermal stability improvement of the

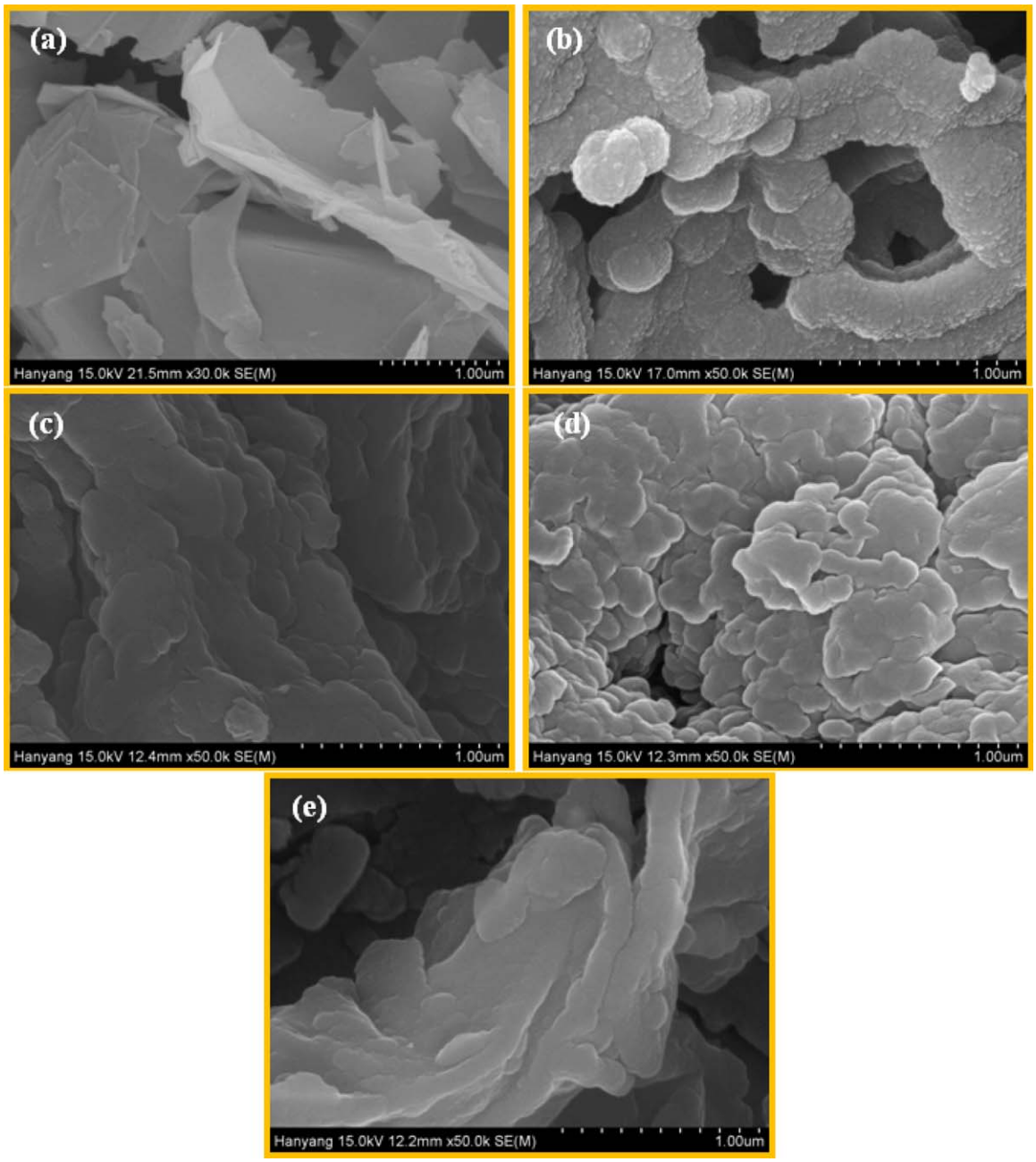

Figure 8. SEM images of GN (a), PPy (b) and PPy/GN composites with GN concentration of 1 wt %, (c) 2 wt % (d), and 5 wt % (e). [Color figure can be viewed in the online issue, which is available at wileyonlinelibrary.com.]

polymer by adding GN in the PPy. The thermal stability of the nanocomposites increased with increasing GN wt %. PPy/GN nanocomposite with 5 wt % GN contents shows the highest thermal stability and total weight loss of ~54% while the sample with 1 wt % revealed a weight loss of ~61%. It is thought that the addition of GN sheets in the polymer restricts the mobility and thermal vibration of PPy chains on the GN-PPy interface and eventually delays the degradation of PPy chains.[18,34] Initial weight loss in the nanocomposites is due to the evaporation of water from the sample. Weight loss around 200°C is due to removal of oxygen containing functional groups in the nanocomposites. Major weight loss in the PPy/GN at ~300–350°C is due to the decomposition of PPy from the nanocomposites.[16,20] Finally, the weight loss in the nanocomposites at ~600°C was ~55, 50, and 45% for the GN wt % 1, 2, and 5, respectively. These results show that GN based PPy nanocomposites exhibit higher thermal stability than pure PPy.

The electrical conductivities of PPy and PPy/GN pellets were measured by the 4-probe method at different pressing pressures ranging from 2 to 8 tons. Figure 10 shows the electrical conductivities of PPy and PPy/GN nanocomposites with different GN wt %. It can be seen that the electrical conductivities of the

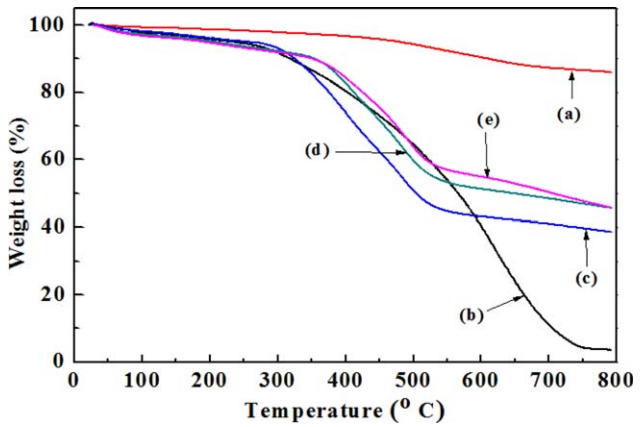

Figure 9. TGA analysis of GN (a), PPy (b) and PPy/GN composites with GN concentration of 1 wt %, (c) 2 wt % (d), and 5 wt % (e). [Color figure can be viewed in the online issue, which is available at wileyonlinelibrary.com.]

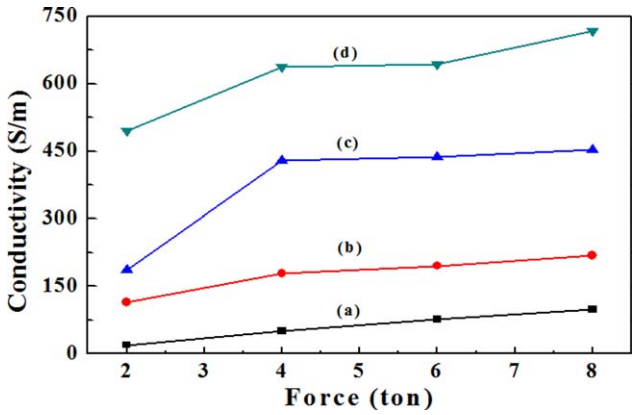

Figure 10. Electrical conductivity of PPy (a) and PPy/GN composites with GN concentration of (b) 1 wt % (b), 2 wt % (c), and 5 wt % (d). [Color figure can be viewed in the online issue, which is available at wileyonlinelibrary.com.]

nanocomposites increased with increasing GN content and pressing pressure. This increase is mainly attributed to the π–π stacking between GN and PPy, high aspect ratio and large surface area of GN in the PPy matrix.[20] It can also be observed that the conductivity of PPy and PPy/GN nanocomposites increased as the applied pressing pressure increases. In case of PPy an electrical conductivity of 19.71 S m^{-1} was registered at the applied pressure of 2 tons which increased significantly to 98.12 S m^{-1} at the pressing pressure of 8 ton. The PPy/GN nanocomposite with GN contents of 5 wt % exhibited the maximum electrical conductivity (717.06 S m^{-1}). These findings demonstrate that through increasing the pressing pressure, voids and entrapped air inside the composite matrix can be eliminated and the nano filler inside the polymer matrix can come close to each other and form an effective conductive path which reduces resistance in the composite structure.[35,36] As a result of this effect, the electrical conductivities of the materials increase with increasing the applied pressure. Figure 10 shows a graphical representation of the electrical conductivities of the pure PPy and PPy/GN nanocomposites with different GN wt %. It can be seen that a sharp increase of material conductivities occurred at the pressing pressure of 4 ton. The electrical conductivities of the samples pressed at applied pressure 6 and 8 ton increased gradually due the fact that the considerable removal of voids and formation of conductive path took place at 4 ton.[36]

Meanwhile, Figure 11 represents the mechanism involved in the formation of nanocomposites with harnessed conductivity as a result of increasing the pressing pressure. A three-dimensional network structure is formed with the addition of GN sheets in the PPy matrix which results in the formation of a conductive path. However when the pressure is applied on the nanocomposites, the GN sheets come close to each other thus increasing the number of conductive paths and subsequently enhancing the electrical conductivity of the PPy/GN nanocomposites. These findings give us an insight into the fact that by increasing the pressing pressure, entrapped air, and voids inside the nanocomposites can be removed and the nanofiller inside the polymer matrix comes close to form effective conductive path and higher values of conductivities can be obtained. Therefore applied pressure, synthetic method and doping of the PPy polymer could collectively be the main factors for harnessing the electrical properties of the nanocomposites. Generally, these factors are seemingly controllable while the synthetic method adopted in the present study is facile and reproducible.

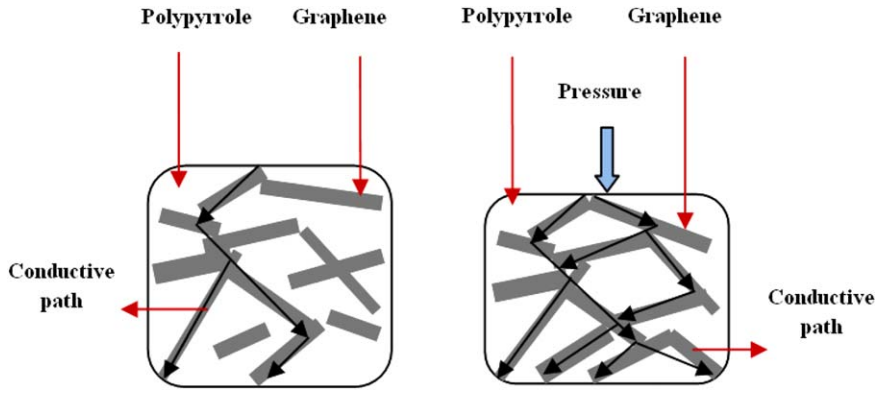

Figure 11. Formation of conductive path in composites by applying pressure. [Color figure can be viewed in the online issue, which is available at wileyonlinelibrary.com.]

Table I. Comparison of the Electrical Conductivities of PPy-Based Composites Obtained at Different Conditions

Report	Sample name	Pressing pressure (ton)	Pressing pressure (MPa)	Measurement temperature (°C)	GN wt %	Conductivity (S m^{-1})
Ref. 12	PPy	-	-	25	-	65
	PPy/GN	-	-	25	50	5000
Ref. 17	PPy	-	0.015	20	-	107
	PPy/GN	-	0.015	20	10	1980
Ref. 37	PPy	-	10	25	-	0.73
	PPy/CNT (23.1 wt %)	-	10	25	-	23
Ref. 16	PPy	2	-	25	-	30
Ref. 20	PPy	-	-	25	-	19
	PPy/GN	-	-	25	25	793
Ref. 19	PPy/PEG[a]	-	-	25	-	9000
Ref. 10	PPy	-	-	20	-	20
This report	PPy	8	-	25	-	98.1
	PPy/GN	8	-	25	5	717.1

[a] Polyethylene glycol.

Based on previous investigations, different nanofillers such as Carbon nanotubes (CNT), graphene oxide (GO) and GN is suitable for enhancing the electrical conductivities of PPy nanocomposites. Table I summarizes the electrical conductivities of PPy and PPy based nanocomposites from various reports. Wang *et al.*[12] used sulfonated GN to synthesize PPy/GN nanocomposites in the presence of ammonium peroxodisulfate. The maximum conductivity of 5000 S m^{-1} was reported for the GN contents as high as 50 wt %. Liu *et al.*[17] reported an electrical conductivity of 1980 S m^{-1} for the PPy/GN nanocomposites with 10 wt % GN contents prepared by *in situ* intercalative chemical polymerization technique. Long *et al.*[37] investigated the electrical conductivity of the PPy/CNT nanocomposite synthesized by an *in situ* chemical oxidative polymerization method. It was observed that the samples with the CNT loading of 23.1 wt % possessed an electrical conductivity of 23 S m^{-1}. These versatile investigations indicate that the electrical properties of conductive polymer based nanocomposites does not only depend upon the kind of dopant/filler but morphology, synthetic method and chain structure of PPy has a profound effect on the conductivity as well.[13] The results of the present study demonstrate that PPy/GN nanocomposites with enhanced electrical conductivities can be fabricated by modified *in situ* EP approach in the presence of DBSA and GN as a dopant. The electrical conductivities of the nanocomposites obtained via this method (at room temperature) were considerably higher than those that have previously been reported. Indeed, the effect of different pressing pressures and the GN contents on the electrical conductivity of PPy/GN nanocomposites has been rarely studied.

CONCLUSIONS

Herein we reported the enhancement of PPy/GN nanocomposites with GN wt % ranging from 1 to 5%. A modified *in situ* EP method was used to synthesize PPy/GN nanocomposites under mild conditions in the presence of DBSA as an emulsifier and doping agent. SEM images showed that the nanocomposites had sheet like morphology. TEM images revealed that PPy was well distributed on the GN surface. From the XRD results, it was concluded that PPy and GN have been completely intercalated and possibly π–π stacking occurs between the PPy chains and GN sheets. UV–vis results also suggested the interaction between PPy and GN. FT-IR and Raman results indicated there was better interaction between the aromatic rings of pyrrole and GN due to better dispersion of GN in PPy and also confirmed the doping of BDSA in PPy. TGA results clearly indicated that the thermal stability of the nanocomposites increased with increasing GN contents. The maximum electrical conductivity (717.06 S/m) was attained in the sample with 5 wt % GN contents and the pressing pressure of 8 tons. This work provides an easy, cheap and reproducible approach for the synthesis of PPy/GN nanocomposites with the tunable properties suitable for various electrochemical and semiconductor applications like supercapacitor electrodes, chemical sensors, and in electronic devices.

ACKNOWLEDGMENTS

The authors are thankful to the Korea Institute of Energy Technology Evaluation and Planning (KETEP) from the Ministry of Trade, Industry and Energy of the Republic of Korea through Human Resources Development Program (Grant No. 20124030200130) for supporting this work.

REFERENCES

1. Xu, C.; Sun, J.; Gao, L. *J. Mater. Chem.* **2011**, *21*, 11253.
2. Amarnath, C. A.; Hong, C. E.; Kim, N. H.; Ku, B.-C.; Kuila, T.; Lee, J. H. *Carbon* **2011**, *49*, 3497.

3. Hsu, F.-H.; Wu, T.-M. *Synth. Met.* **2012**, *162*, 682.
4. Geim, A. K.; Novoselov, K. S. *Nat. Mater.* **2007**, *6*, 183.
5. Imran, S.; Kim, Y.; Shao, G.; Hussain, M.; Choa, Y.-H.; Kim, H. *J. Mater. Sci.* **2013**, *49*, 1328.
6. Peighambardoust, S. J.; Pourabbas, B. *Macromol. Symp.* **2007**, *247*, 99.
7. Han, D.; Chu, Y.; Yang, L.; Liu, Y.; Lv, Z. *Colloids Surf. A* **2005**, *259*, 179.
8. Moiz, S. A.; Imran, S. M.; Kim, S. M.; Nahhas, A. M.; Kim, H. T. *Optoelectron. Adv. Mater. Rapid Commun.* **2012**, *6*, 1113.
9. Lim, S. P.; Pandikumar, A.; Lim, Y. S.; Huang, N. M.; Lim, H. N. *Sci. Rep.* **2014**, *4*, 5305.
10. Yamamoto, M. A. A. H. *Polym. J.* **2006**, *38*, 703.
11. Manivel, P.; Kanagaraj, S.; Balamurugan, A.; Ponpandian, N.; Mangalaraj, D.; Viswanathan, C. *Colloids Surf. A* **2014**, *441*, 614.
12. Wang, X.; Yang, C.; Li, H.; Liu, P. *Electrochim. Acta* **2013**, *111*, 729.
13. Košina, S.; Balúch, S.; Annus, J.; Omastová, M.; Krištín, J. *J. Mater. Sci.* **1994**, *29*, 3403.
14. Kuilla, T.; Bhadra, S.; Yao, D.; Kim, N. H.; Bose, S.; Lee, J. H. *Prog. Polym. Sci.* **2010**, *35*, 1350.
15. Zhang, K.; Zhang, L. L.; Zhao, X. S.; Wu, J. *Chem. Mater.* **2010**, *22*, 1392.
16. Konwer, S.; Boruah, R.; Dolui, S. *J. Electron. Mater.* **2011**, *40*, 2248.
17. Liu, Y.; Wang, H.; Zhou, J.; Bian, L.; Zhu, E.; Hai, J.; Tang, J.; Tang, W. *Electrochim. Acta* **2013**, *112*, 44.
18. Sahoo, S.; Karthikeyan, G.; Nayak, G. C.; Das, C. K. *Synth. Met.* **2011**, *161*, 1713.
19. Kang, H. C.; Geckeler, K. E. *Polymer* **2000**, *41*, 6931.
20. Bose, S.; Kuila, T.; Uddin, M. E.; Kim, N. H.; Lau, A. K. T.; Lee, J. H. *Polymer* **2010**, *51*, 5921.
21. Zhao, Y.; Zhan, L.; Tian, J.; Nie, S.; Ning, Z. *Electrochim. Acta* **2011**, *56*, 1967.
22. Fan, Y.; Liu, Y.; Cai, Q.; Liu, Y.; Zhang, J. *Synth. Met.* **2012**, *162*, 1815.
23. Lin, W.-D.; Chang, H.-M.; Wu, R. *J. Sens. Actuat. B* **2013**, *181*, 326.
24. Kotal, M.; Srivastava, S. K.; Paramanik, B. *J. Phys. Chem. C* **2011**, *115*, 1496.
25. Huang, Q.; Zeng, D.; Tian, S.; Xie, C. *Mater. Lett.* **2012**, *83*, 76.
26. Gao, Y.-S.; Xu, J.-K.; Lu, L.-M.; Wu, L.-P.; Zhang, K.-X.; Nie, T.; Zhu, X.-F.; Wu, Y. *Biosens. Bioelectron.* **2014**, *62*, 261.
27. Liu, J.; An, J.; Ma, Y.; Li, M.; Ma, R. *J. Electrochem. Soc.* **2012**, *159*, A828.
28. Botta, C.; Mercogliano, C.; Bolognesi, A.; Majumdar, H. S.; Pal, A. *J. Appl. Phys. Lett.* **2004**, *85*, 2393.
29. Ruiz Peralta, M. D. L.; Pal, U.; Zeferino, R. S. *ACS Appl. Mater. Interfaces* **2012**, *4*, 4807.
30. He, C. J.; San, P. S.; Pei, K. *Sci. Rep.* **2013**, 3, 2144.
31. Lv, X.-J.; Zhou, S.-X.; Zhang, C.; Chang, H.-X.; Chen, Y.; Fu, W.-F. *J. Mater. Chem.* **2012**, *22*, 18542.
32. Shen, Y.; Wan, M. *Synth. Met.* **1998**, *96*, 127.
33. Yu, L.; Zhang, Y.; Tong, W.; Shang, J.; Lv, F.; Chu, P. K.; Guo, W. *Compos. A* **2012**, *43*, 2039.
34. Lozano, K.; Barrera, E. V. *J. Appl. Polym. Sci.* **2001**, *79*, 125.
35. Hussain, M.; Choa, Y.-H.; Niihara, K. *Compos. A* **2001**, *32*, 1689.
36. Zhang, D. *Polym. Test.* **2007**, *26*, 9.
37. Yunze, L. Z. C.; Xuetong, Z.; Jin, Z.; Zhongfan, L. *J. Phys. D Appl. Phys.* **2004**, *37*, 1965.